The EMBO Journal Vol. 21 No. 6 pp. 1339–1349, 2002

Arabidopsis FHY3 defines a key phytochrome A signaling component directly interacting with its homologous partner FAR1

Haiyang Wang and Xing Wang Deng[1]

Department of Molecular, Cellular and Developmental Biology, Yale University, New Haven, CT 06520-8104, USA

[1]Corresponding author
e-mail: xingwang.deng@yale.edu

In *Arabidopsis*, phytochrome A (phyA) is the primary photoreceptor mediating various plant responses to far-red (FR) light. Here we show that phyA signaling involves a combinatorial action of downstream intermediates, which controls overlapping yet distinctive sets of FR responses. FHY3 is a prominent phyA signaling intermediate sharing structural similarity to FAR1, a previously identified phyA signaling component. The *fhy3* and *far1* mutants display similar yet distinctive defects in phyA signaling; however, overexpression of either FHY3 or FAR1 suppresses the mutant phenotype of both genes. Moreover, overexpression of partial fragments of FHY3 can cause a dominant-negative interference phenotype on phyA signaling that is stronger than those of the *fhy3* or *far1* null mutants. Further, we demonstrate that FHY3 and FAR1 are capable of homo- and hetero-interaction. Our data indicate that FHY3, together with FAR1, defines a key module in a signaling network underlying phyA-mediated FR light responses.

Keywords: *Arabidopsis*/FAR1/FHY3/light signaling/phytochrome

Introduction

Plants adjust their growth and development according to their light environment through a network of photoreceptors. Among them, the phytochromes (phys) are best characterized and exist in two distinct but photoconvertible forms, the red (R)-absorbing Pr and the far-red (FR)-absorbing Pfr (Neff *et al*., 2000; Wang and Deng, 2002). In *Arabidopsis*, there are five distinct phytochromes, designated phyA–E. These photoreceptors have unique, sometimes partially redundant, or antagonistic roles in different photomorphogenic responses (Deng and Quail, 1999). phyA is the primary photoreceptor mediating the high irradiance response (HIR) to continuous FR light (FRc), including inhibition of hypocotyl elongation, opening of the apical hook, expansion of cotyledons, accumulation of anthocyanin and FRc preconditioned blocking of greening (Nagatani *et al*., 1993; Whitelam *et al*., 1993). In addition, phyA is also the photoreceptor responsible for the very low fluence response (VLFR; Yanovsky *et al*., 1997) and for the regulation of many light-responsive genes by FR light, such as *CAB* (chlorophyll *a/b* binding protein), *RBCS* (small subunit of ribulose-1,5-bisphosphate carboxylase), *CHS* (chalcone synthase) and *PORA* (NADPH:Pchlide oxidoreductase A) (Kuno and Furuya, 2000; Ma *et al*., 2001).

Recent molecular genetic studies have greatly enhanced our understanding of phyA signaling, particularly towards identifying the molecular components potentially involved in the early steps of the signaling pathway linking phyA to light-responsive gene expression and photomorphogenic development. Both general screenings for phytochrome-interacting partners and targeted protein–protein interaction studies have identified a number of phytochrome-interacting factors. These include PIF3 (a nuclear bHLH protein), PKS1 (a cytoplasmic substrate for the kinase activity of phytochrome), NDPK2 (nucleoside diphosphate kinase 2), cryptochromes (both CRY1 and CRY2) and the AUX/IAA proteins (Colón-Carmona *et al*., 2000; Quail, 2000). One school of thought suggests that light signals could activate the kinase activity of phytochromes, which phosphorylate themselves and their interacting partners to initiate a signaling cascade (Fankhauser, 2000). On the other hand, genetic analyses have led to the identification and subsequent molecular characterization of a number of phyA signaling intermediates (Hudson, 2000). Several positive regulators have been defined, including both cytosolic and nuclear proteins. For example, LAF6 is a plastid-localized ATP-binding cassette protein involved in coordinating intercompartmental communication between plastids and the nucleus (Møller *et al*., 2001). PAT1 and FIN219 are cytoplasmic proteins (Bolle *et al*., 2000; Hsieh *et al*., 2000), whereas FHY1, FAR1, HFR1 and LAF1 are nuclear-localized factors (Hudson *et al*., 1999; Fairchild *et al*., 2000; Ballesteros *et al*., 2001; Desnos *et al*., 2001). LAF1 is a MYB-type transcription activator, whereas HFR1 is a bHLH-type transcription factor capable of heterodimerizing with PIF3. Two negative regulators, SPA1 and EID1, have also been defined and shown to be nuclear-localized factors (Hoecker *et al*., 1999; Dieterle *et al*., 2001). EID1 is a novel F-box protein probably involved in ubiquitin-dependent proteolysis. The biochemical functions of other components remain largely unknown.

Here we report a detailed genetic and physiological study to characterize the relationships between various genetically defined phyA signaling intermediates. Our data support the notion that phyA signaling involves multiple early intermediates that control overlapping yet distinctive sets of FRc responses. *FHY3* (far-red elongated hypocotyl 3) represents one of the early signal transducers of phyA signaling. Loss-of-function *fhy3* mutant retains most VLFR responses but is severely impaired in the FR–HIR responses, including hypocotyl growth, cotyledon unfolding, anthocyanin accumulation and FRc preconditioned block of greening (Yanovsky *et al*., 2000). Molecular cloning of *FHY3* revealed that it encodes a nuclear protein

Table I. Summary of *fhy3* mutants used in this study

Allele no.	Isolate name	Ecotype	Molecular lesion
fhy3-1	*fhy3*	Col	R91*
fhy3-2	128	Col	ND
fhy3-3	CS6474	WS	360QYTALPFSLACIDEGF*
fhy3-4	8RF4	No-0	W501*
fhy3-5	17FR2	No-0	W171*
fhy3-6	19FR9	No-0	Q607*
fhy3-7	20FR1	No-0	W269*
fhy3-8	25FR14	No-0	ND
fhy3-9	41FR4	No-0	G305R
fhy3-10	42FR1	No-0	D283N

ND, not determined. Asterisks designate stop codons.

highly similar to FAR1, a previously identified phyA signaling intermediate. We present genetic and molecular evidence to support the view that FHY3, together with FAR1, defines a key module in the phyA signaling network mediating various FRc responses.

Results

Isolation of additional fhy3 mutant alleles

To identify new components in the phyA signaling pathway, we screened two independent T-DNA mutated *Arabidopsis* populations under FRc to select mutants with elongated hypocotyls (see Materials and methods). A number of mutants were identified and subjected to genetic complementation tests with previously identified mutants of similar phenotype. Two new mutations were found to be allelic to the previously identified *fhy3* mutant (designated *fhy3-1*; Whitelam *et al*., 1993) and were designated *fhy3-2* and *fhy3-3*. Seven additional new alleles (designated *fhy3-4 to fhy3-10*) were isolated in a previous screen for the *far1* mutants and kindly provided by Dr Quail's group (Table I; Hudson *et al*., 1999).

When compared with wild-type (WT) seedlings, the *fhy3* mutants display a long-hypocotyl phenotype and reduced cotyledon expansion under FRc but no significant phenotypes under continuous red (R) or blue light (B) (Figures 1A–C and 2A). There are no observable defects when the seedlings are grown in the dark or under white light (data not shown), indicating that the *fhy3* mutant phenotype is light dependent and specific to FRc. This FRc phenotype is not due to reduced levels of active phyA or to a deficiency in chromophore biosynthesis (Whitelam *et al*., 1993). Thus, FHY3 likely represents a signaling intermediate for phyA.

Genetic analyses indicate no simple downstream/upstream relationships among phyA signaling components

Among the previously identified phyA signaling mutants, *fhy1*, *fhy3*, *far1* and *fin219* display elongated hypocotyls under FRc (Whitelam *et al*., 1993; Hudson *et al*., 1999; Hsieh *et al*., 2000), and *fhy3* exhibits the most pronounced long-hypocotyl phenotype under our growth condition. On the other hand, the *spa1* mutants have an increased sensitivity to FRc and shorter hypocotyls (Hoecker *et al*., 1998; Figures 1D and 2B). To examine the genetic relationships among these loci, selective pair-wise double

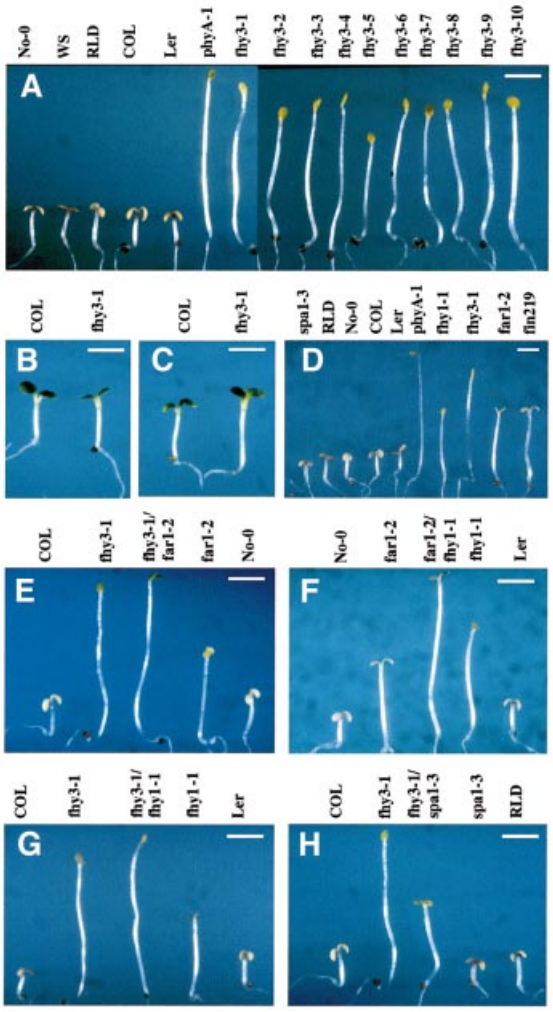

Fig. 1. Phenotype of *fhy3* and double-mutant analysis of FR specific mutants. (**A**) *fhy3* mutants (10 alleles) are deficient in FRc-induced inhibition of hypocotyl elongation and cotyledon expansion. Also shown are seedlings of five ecotypes of WT *Arabidopsis* and the *phyA-1* mutant. (**B**) *fhy3-1* grown under R light (compared with its corresponding ecotype Col). (**C**) *fhy3-1* grown under B light. (**D**) Far-red grown seedling phenotypes of five FRc specific mutants (*spa1-3, fhy1-1, fhy3-1, far1-2* and *fin219*) compared with their corresponding ecotypes and the *phyA-1* mutant. (**E–G**) The *fhy3-1/far1-2*, *far1-2/fhy1, fhy3-1/fhy1* double mutants display longer hypocotyls and less-unfolded cotyledons than their parental mutants. (**H**) The *fhy3-1/spa1-3* double mutant has an intermediate length of hypocotyl. Scale bar in all panels: ~2 mm.

mutants were constructed, and their light-dependent phenotypes were examined and compared with their respective parental mutants and WT controls.

As shown in Figures 1E–G and 2C, under a high fluence rate of FRc, *fhy3-1/far1-2*, *far1-2/fhy1-1* and *fhy3-1/fhy1-1* double mutants possess longer hypocotyls and further reduced expansion of cotyledons compared with their respective single parental mutants. This result indicates that these mutations have additive effects in phyA signaling, suggesting that they may act in a parallel fashion. It should be noted that these double mutants have a reduced but not a complete loss of sensitivity to FRc. On the other hand, the *fhy3-1/spa1-3* double mutant displays a hypocotyl of intermediate length under FRc (Figures 1H and 2C), indicating that these two mutations

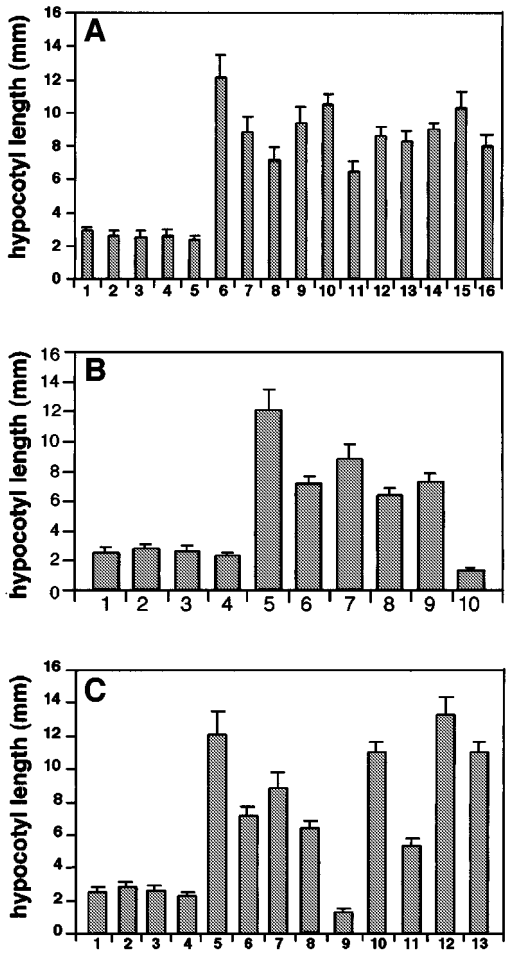

Fig. 2. Quantitative analysis of the hypocotyl length of *Arabidopsis* phyA signaling mutants and double mutants. (**A**) Ten alleles of *fhy3* mutants, *phyA-1* and their corresponding ecotypes: (1) No-0, (2) WS, (3) RLD, (4) Col, (5) Ler, (6) *phyA-1*, (7) *fhy3-1*, (8) *fhy3-2*, (9) *fhy3-3*, (10) *fhy3-4*, (11) *fhy3-5*, (12) *fhy3-6*, (13) *fhy3-7*, (14) *fhy3-8*, (15) *fhy3-9*, (16) *fhy3-10*. The error bars represent the standard deviations. (**B**) phyA signaling mutants and their corresponding ecotypes: (1) RLD, (2) No-0, (3) Col, (4) Ler, (5) *phyA-1*, (6) *fhy1-1*, (7) *fhy3-1*, (8) *far1-2*, (9) *fin219*, (10) *spa1-3*. The error bars represent the standard deviations. (**C**) The phyA signaling mutants, double mutants and their respective ecotypes: (1) RLD, (2) No-0, (3) Col, (4) Ler, (5) *phyA-1*, (6) *fhy1-1*, (7) *fhy3-1*, (8) *far1-2*, (9) *spa1-3*, (10) *fhy3-1/far1-2*, (11) *fhy3-1/spa1-3*, (12) *fhy3-1/fhy1-1*, (13) *far1-2/fhy1-1*. The error bars represent the standard deviations.

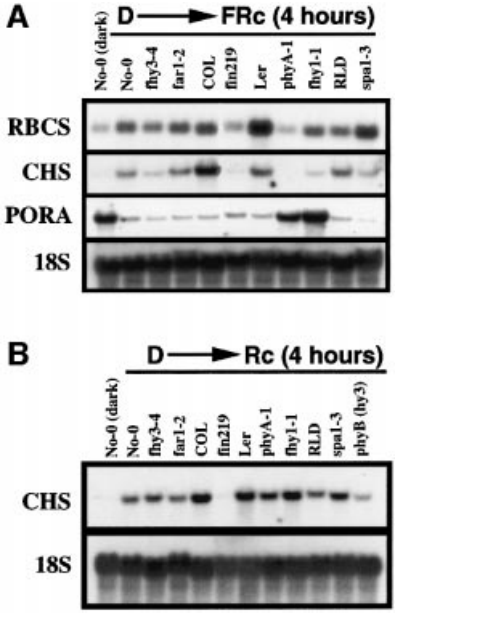

Fig. 3. RNA gel blot analysis of light-regulated gene expression in phyA signaling mutants. *fhy3-4* and *far1-2* are in No-0 ecotype background. *fin219* is in COL ecotype background. *phyA-1*, *fhy1-1* and *hy3* (*phyB*) are in Ler ecotype background. *spa1-3* is in RLD ecotype background. For the dark control experiment, only No-0 ecotype is shown, as the expression of *RBCS*, *CHS* and *PORA* is of similar levels in these four different ecotype WT seedlings. (**A**) Effects of *fhy3* and other FR signaling mutants on FR induction (4 h) of *RBCS*, *CHS*, and FR repression of *PORA*. An 18S rRNA was used as the loading control. (**B**) Effects of *fhy3* and other FR specific signaling mutants on R induction (4 h) of *CHS*.

can compensate each other to some extent. This suggests that there may be no simple downstream/upstream relationship between *FHY3* and *SPA1*. We also examined these double mutants under a wide range of FRc fluence rates, and similar effects were observed to those shown in Figure 1E–H, although the differences become less pronounced under low fluence rate irradiations (data not shown). In addition, these double mutants display essentially normal responses to R and B light conditions (data not shown).

Light-regulated gene expression in fhy3 and other phyA signaling mutants

To explore the molecular basis for the developmental defects, we examined the changes in three representative phyA-dependent gene expression patterns (*RBCS*, *CHS*, *PORA*) in *fhy3-4* and the following available phyA signaling mutants: *phyA-1*, *fhy1-1*, *far1-2*, *fin219* and *spa1-3*. Seedlings were grown under darkness for 4 days prior to illumination with 4 h of FRc. As shown in Figure 3A, WT seedlings show a clear induction of *RBCS* and *CHS*, while the expression of *PORA* is significantly suppressed. The induction of both *RBCS* and *CHS* is almost completely abolished in *phyA-1*, *fin219* and *fhy1-1*, and is severely attenuated in *fhy3-4*. No obvious effect was found in *far1-2* (Figure 3A). Notably, *RBCS* induction is clearly enhanced in *spa1-3*, while the induction of *CHS* seems impaired under this condition (Figure 3A). However, *CHS* expression is increased in FRc-grown *spa1-3* seedlings (data not shown), consistent with the observed increasing accumulation of anthocyanin in this mutant (Hoecker *et al*., 1998). The repressive effect of FRc on *PORA* expression is severely compromized in *phyA-1* and *fhy1-1*, but apparently normal in all other mutant backgrounds examined (Figure 3A).

Previously it has been shown that phyA is also involved in R-mediated *CHS* induction (Barnes *et al*., 1996a), therefore we also examined the effects of *fhy3* and various phyA signaling mutants on this response. Similarly, seedlings were grown under darkness for 4 days prior to illumination with 4 h of continuous R. As shown in Figure 3B, *CHS* induction is dramatically reduced in *phyB* and slightly impaired in *phyA-1*, indicating that both phyA and phyB are involved in R-mediated induction of *CHS* expression, with phyB playing a major role in this

response. Interestingly, this response is almost completely abolished in *fin219* and is slightly increased in *spa1-3*. The effects of *fhy3-4*, *fhy1-1* and *far1-2* on this response are minimal.

FHY3 encodes a protein related to FAR1

Although two new *fhy3* alleles (*fhy3-2* and *fhy3-3*) were identified from two independent T-DNA mutagenesis populations, co-segregation tests show that neither mutation is linked to the T-DNA insertion (data not shown). Therefore, we generated an F_2 mapping population by crossing the *fhy3-2* allele (*COL* ecotype) to WT ecotype *Ler*. We mapped the *FHY3* locus to a region of chromosome III between the SSLP markers *nga162* and *GAPab* (Konieczny and Ausubel, 1993; Bell and Ecker, 1994). Further mapping with several newly developed SSLP, CAP and RFLP markers delimited *FHY3* to the region flanked by two RFLP markers, *mi142* and *mi268*. A set of BAC clones covering this genomic region was obtained from the *Arabidopsis* stock center. New RFLP markers were developed from these BAC clones and used to further locate the *FHY3* locus to a single BAC clone, F2F24 (Figure 4A).

The F2F24 BAC clone was used to screen an *Arabidopsis* cDNA library derived from dark-grown seedlings and four different types of cDNA were isolated. Sequence analysis revealed that one of the cDNAs encodes a protein with similarity to FAR1, a nuclear protein required for phyA signaling (Hudson *et al*., 1999). Thus, we sequenced the genomic region of this gene for eight *fhy3* alleles. In each case, a single mutation in the putative open reading frame was identified (Table I), providing convincing evidence that this cDNA clone defines the *FHY3* gene. Comparison of the cDNA with the genomic sequence revealed that the *FHY3* gene is composed of eight exons and seven introns (Figure 4B).

FHY3, together with FAR1, FRS1–FRS3 (Hudson *et al*., 1999) and eight new members designated FRS4–FRS11, comprise a multigene family present in the *Arabidopsis* genome. Interestingly, FHY3 and FAR1 share the highest homology (50% identity and 75% similarity) to each other and they compose a branch of this gene family (Figure 4C). Moreover, similar proteins have also been identified in other plant species, including monocotyledon plants (Hudson *et al*., 1999), indicating that this family of genes is conserved throughout the evolution of the plant kingdom.

The *FHY3* cDNA encodes a predicted polypeptide of 839 amino acids, identical to that of AT3g22170 annotated through the *Arabidopsis* genome project and with a secondary structure similar to FAR1 (Hudson *et al*., 1999). The residues between 603 and 699 are predicted to form a coiled-coil motif. In addition, FHY3 contains a basic region (**KKK**NPT-**KKRK**, residues 709–718, basic residues in bold), which could act as a nuclear localization signal (NLS) (Figure 4D). However, it should be pointed out that putative NLS motifs are only identified in some of the family members, such as FAR1, FHY3 and FRS2, but not in others, such as FRS1 and FRS3. Furthermore, these proteins may also differ in their secondary structures, as some members (such as FRS3) lack the coiled-coil domain identified in the C-termini of both FHY3 and FAR1, whereas other members possess multiple coiled-coil domains (such as FRS1 and FRS2). These features suggest that those family members may have overlapping as well as distinct functions.

FHY3 expression is regulated by phyA signaling

To determine whether the expression of *FHY3* is light dependent, and also its dependence on phyA, we examined *FHY3* transcript levels in dark- and FRc-grown WT seedlings as well as in selected FRc-grown phyA signaling mutant seedlings. In WT seedlings, the *FHY3* transcript level is clearly reduced by FRc treatment as compared with dark treatment. For FRc-grown seedlings, the *FHY3* transcript level is dramatically reduced in *fhy3-1*, *fin219* and *spa1-3*, but is significantly increased in *far1-2* (Figure 5A), indicating that the expression of *FHY3* is subject to regulation by phyA and its signaling intermediates FIN219, SPA1 and FAR1.

Overexpression of either FHY3 or FAR1 suppresses the mutant phenotype of both genes

The high homology shared by FHY3 and FAR1 and their similar mutant phenotypes suggest that these two genes may have similar functions. To examine this possibility, we introduced a 35S promoter-driven myc epitope-tagged *FHY3* cDNA transgene (*myc-FHY3*) or a myc-flag-HA (MFH) epitope-tagged *FAR1* cDNA transgene (*MFH-FAR1*; Figure 5B) into both *fhy3-1* and *far1-2*. As expected, a functional complementation of each parental mutant by overexpressing its corresponding gene was observed (Figures 5C, a and c, and 6G). We also observed an apparent suppression of the mutant phenotype by overexpressing the homologous gene (Figures 5C, b and d, and 6G). It should be noted that we did not observe a strongly enhanced FRc response when the same transgenes were introduced into a WT background, nor was a suppression effect detected when the same transgenes were introduced into other FRc-specific long-hypocotyl mutants such as *fhy1* and *fin219* (data not shown). Moreover, dark-grown seedlings overexpressing FHY3 and FAR1 do not exhibit any detectable phenotypes (data not shown), suggesting that these two proteins share a bona fide functional overlap and that their activation requires activated phyA.

FHY3 protein is constitutively nuclear localized

To determine the subcellular localization of FHY3, the full-length *FHY3* cDNA was translationally fused to the 3′ end of the *GUS* reporter gene under the control of the strong 35S promoter (*GUS-FHY3*; Figure 5B). The transgene successfully rescued the *fhy3* mutant phenotype (Figure 5C, e and f). In the rescued transgenic plants, the GUS–FHY3 fusion protein is exclusively found in the nucleus under both dark and FRc treatment (Figure 5D, a and b). This localization pattern is similar to that of a constitutive nuclear protein, GUS–NIa (Figure 5D, c and d), indicating that FHY3 is a constitutive nuclear protein.

Dominant-negative effect of overexpressing partial fragments of FHY3

To examine the structure–function relationship of FHY3, we generated transgenic plants overexpressing either the N-terminal (N1–541) or C-terminal (C473–839) portions of FHY3 (Figure 5B) in a WT background (*COL* ecotype).

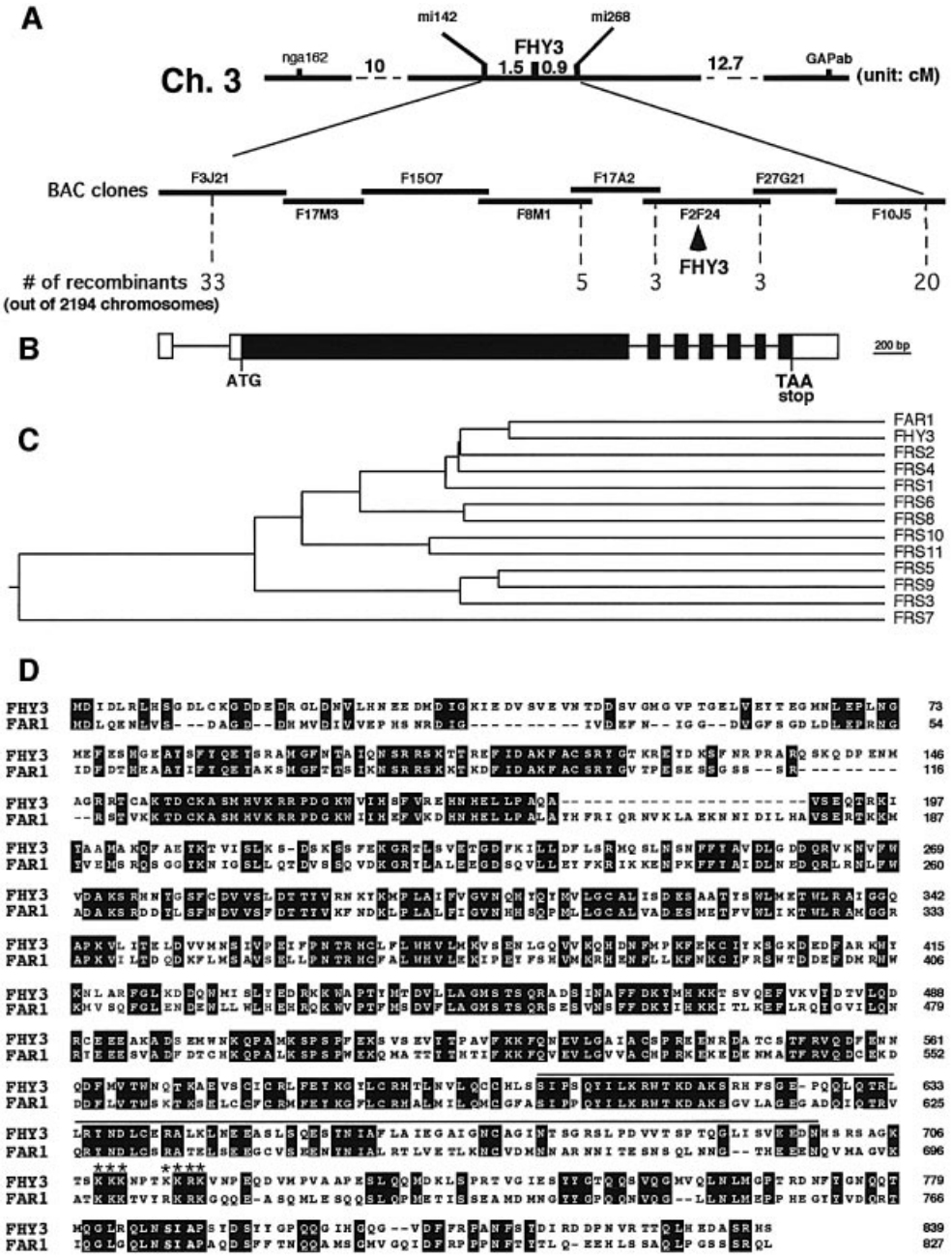

Fig. 4. Cloning and molecular characterization of the *FHY3* gene. (**A**) Cloning of *FHY3* by chromosomal walking. *FHY3* was initially mapped to the top arm of chromosome 3 between the SSLP markers *nga162* and *GAPab*, and further narrowed down to a region flanked by two RFLP markers, *mi142* and *mi268*. A BAC clone contig was established and new RFLP markers were developed to continue the walk. The *FHY3* gene was eventually located to a single BAC clone, F2F24. (**B**) Genomic structure of the *FHY3* gene. The exons (white boxes denote the 5′- and 3′-untranslated regions; black boxes denote the protein coding sequence) are shown as boxes and introns as lines. The start and stop codons are indicated. (**C**) Phylogenetic tree of the *FHY3* gene family, which is composed of 13 members. FHY3 shares highest homology with FAR1 (AF159587). These homologous genes are distributed on all five chromosomes of *Arabidopsis*. FRS1 (T04883), FRS5 (T05645) and FRS9 (T05644) are located on chromosome 4 (BAC F18F4 for FRS1 and BAC F20D10 for both FRS5 and FRS9). FRS2 (AC005700) and FRS3 (AC005623) are located on chromosome 2 (BACs T32F6 and T20P8, respectively). FRS4 (AC012394), FRS6 (AC008016), FRS8 (AC011717) and FRS11 (AC005489) are located on chromosome 1 (BAC F15M4 for FRS4, BAC F6D8 for FRS6, BAC F19K16 for FRS8, F14N23 for FRS11). FRS7 (AC018907) is located on chromosome 3 (BAC F28L1). FRS10 (AF262043) is located on chromosome V (BAC T26D3). The plot was obtained by the Jotun hein algorithm of the Megalign program (DNAstar, Madison, WI). (**D**) Sequence alignment of FHY3 and FAR1. Identical residues are shaded. The predicted coiled-coil region of FHY3 is highlighted by a single line at the top. The stars denote the residues for the putative NLS.

As shown in Figure 6A and B, heterozygous transgenic plants harboring a single T-DNA insertion of the transgene (either N1–541 or C473–839) produce offspring segregating in a 1:2:1 ratio of long-, medium- and short-hypocotyl seedlings. These long-hypocotyl plants are homozygous transgenic plants, the medium ones are heterozygous for the transgene and the short ones are non-transgenic WT plants. This result suggests that these transgenes cause a

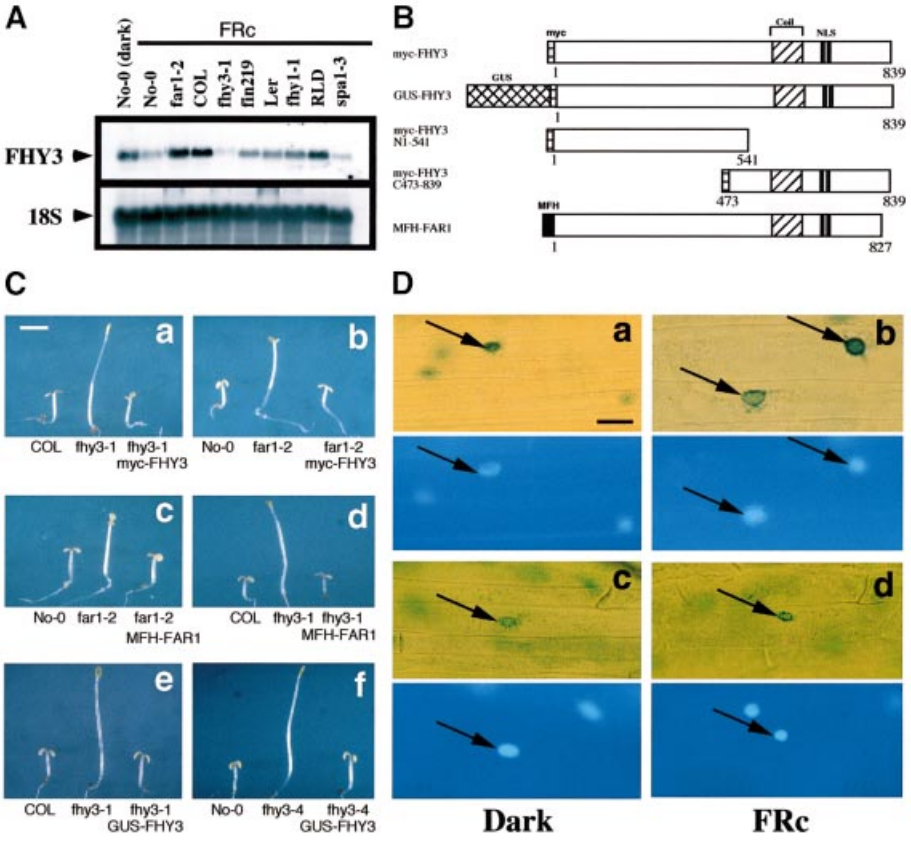

Fig. 5. *FHY3* expression, overexpression and FHY3 protein localization. (**A**) RNA gel blot analysis of *FHY3* expression in dark- and FRc-grown WT seedlings as well as in various FRc-grown mutant seedlings. (**B**) Diagram of the constructs used in plant transformation experiments. The predicted coiled-coil region and the NLS of FHY3, the myc and myc-flag-HA (MFH) epitopes and the *GUS* gene coding region are indicated. (**C**) Overexpression of myc-FHY3 and MFH-FAR1. The *fhy3* and *far1* mutant phenotypes are rescued by overexpressing the corresponding gene (a and c) and suppressed by overexpressing the homologous gene (b and d). GUS-FHY3 also rescues the *fhy3* mutant phenotype (e and f). All panels were taken at the same magnification. Scale bar: ~2 mm. (**D**) Subcellular localization of the FHY3 protein in the *Arabidopsis* hypocotyl cells. Each panel is composed of two portions. The upper portions are the GUS staining of GUS–FHY3 (a and b) and GUS–NIa (c and d). The lower portions are DAPI staining of the corresponding images to show the positions of the nuclei (indicated by arrows). The left panels are from dark-grown seedlings and the right panels from FRc-grown seedlings. All panels were taken at the same magnification. Scale bar: ~50 μm.

dosage-dependent dominant-negative effect on phyA-mediated inhibition of hypocotyl elongation in response to FRc. Notably, homozygous transgenic seedlings overexpressing the C-terminal portion of FHY3 (the E7 line) display a completely etiolated phenotype under FRc, indistinguishable from the phenotype of the *phyA-1* null mutant (Figure 6C, D and G). The same plants have an essentially normal response to R and a slightly reduced response to B light (Figure 6E and F). This result indicates that overexpression of the FHY3 C-terminal fragment in the homozygous seedlings not only impaired the endogenous FHY3 function but also completely blocked phyA signaling. It is plausible that the overabundant mutated form of FHY3 titrated out all normal FHY3 interactive partners and thus completely blocked phyA signaling. This would be consistent with a critical role of FHY3 in the phyA signaling network.

FHY3 and FAR1 interact in a yeast two-hybrid assay and in planta

The structural similarity and genetic interactions between FHY3 and FAR1 prompted us to examine their possible protein–protein interaction. We first examined the FAR1 and FHY3 interaction using a yeast two-hybrid assay. Both genes were cloned into the yeast vectors as fusion proteins with the LexA DNA-binding domain and the GAL4 activation domain (AD; Ausubel *et al*., 1999). As shown in Figure 7A–C, although both LexA–FHY3 and LexA–FAR1 can auto-activate the β-galactosidase reporter gene to certain extents, when combined with AD–FHY3 or AD–FAR1, the activities of the reporter gene are significantly increased (3- to 5-fold). In addition, a C-terminal fragment of FHY3 (amino acids 541–839) containing the coiled-coil domain retains the ability to interact with FAR1, although at a reduced strength. These data suggest that FHY3 and FAR1 are capable of forming homocomplexes with themselves or heterocomplexes with one another.

To substantiate the physical interaction between FHY3 and FAR1, we conducted an *in vivo* co-immunoprecipitation assay with F_2 plants from a cross of GUS–FHY3 and MFH–FAR1 transgenic plants. As shown in Figure 7D, a western blot probed with a GUS antibody detected the GUS–FHY3 fusion protein from the total extract of the F_2 seedlings and F_2 seedlings subjected to immunoprecipitation with either a myc- or a flag-epitope antibody.

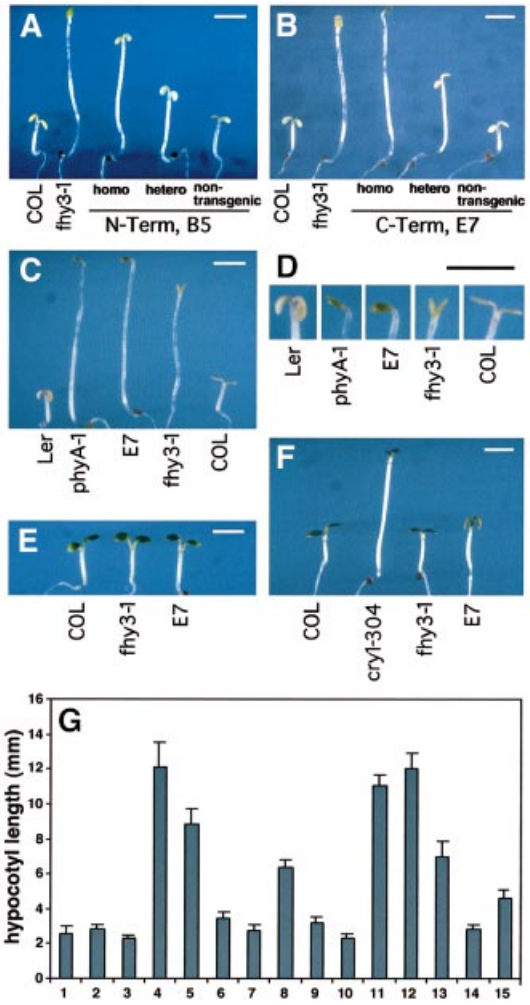

Fig. 6. Dominant-negative effect caused by overexpressing partial fragments of FHY3. (**A** and **B**) The T_2 generation of the transgenic lines B5 (a representative myc-FHY3N1–541 line) and E7 (a representative myc-FHY3C473–839 line) segregate homozygotes (homo), heterozygotes (hetero) and non-transgenic seedlings. The genotypes of the seedlings are determined by drug-resistance tests and the phenotypic segregation ratios of their T_3 generation seedlings. (**C**) Comparison of the homozygote seedlings of E7 with *phyA-1* and *fhy3-1*. Also shown are their respective WT ecotype seedlings. (**D**) Close-ups of the cotyledons for seedlings shown in (C). (**E**) E7 homozygote seedlings respond normally to R. (**F**) E7 homozygote seedlings have marginally elongated hypocotyls under B light. Scale bars: ~2 mm. (**G**) Quantitative analysis of hypocotyl length of various transgenic lines compared with the mutants and wild-type controls: (1) Col, (2) No-0, (3) Ler, (4) *phyA-1*, (5) *fhy3-1*, (6) *fhy3-1, myc-FHY3*, (7) *fhy3-1, MFH-FAR1*, (8) *far1-2*, (9) *far1-2, MFH-FAR1*, (10) *far1-2, myc-FHY3*, (11) *fhy3-1/far1-2*, (12) E7, homozygotes, (13) E7, heterozygotes, (14) E7, segregated non-transgenic seedlings, (15) N-terminal, B5 homozygotes.

However, GUS–FHY3 fusion protein was not detectable from the total extract of wild-type seedlings or from immunoprecipitated F_2 seedlings processed without adding the antibodies. The MFH–FAR1 fusion protein was also detected from the same immunoprecipitated samples on a separate western blot probed with a flag antibody, suggesting a physical association of FHY3 and FAR1 *in planta*. The inability to observe the MFH–FAR1 fusion protein in the total extract of F_2 seedlings with the flag antibody at the same exposure is due to the low expression level of the tagged protein in the total extract.

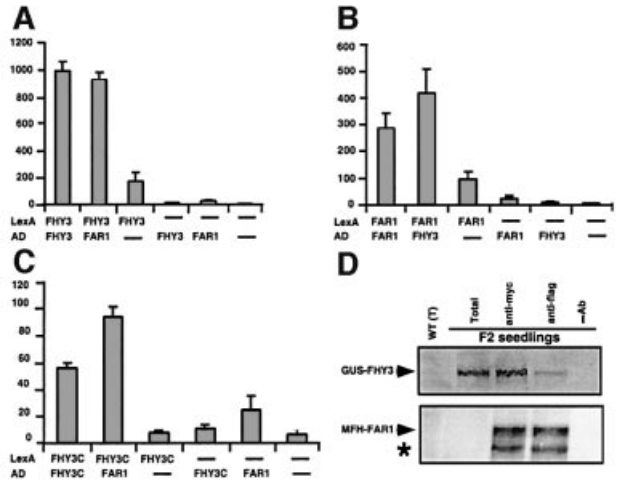

Fig. 7. Direct interaction between FHY3 and FAR1. (**A**–**C**) Quantitative analyses of the relative β-galactosidase activities for the yeast two-hybrid assay. The LexA and AD fusion constructs used in the assay are shown at the bottom of each panel. Unless otherwise indicated, full-length proteins were used. The '—' signs represent the empty vector controls. (**A**) FHY3 interacts with itself and with FAR1. (**B**) FAR1 interacts with itself and with FHY3. (**C**) An FHY3 C-terminal fragment (FHY3C, amino acids 541–839) interacts with FAR1. (**D**) Co-immunoprecipitaion of GUS–FHY3 and MFH–FAR1. Light-grown F_2 seedlings harboring both GUS–FHY3 and MFH–FAR1 were subjected to an immunoprecipitation procedure with either myc or flag monoclonal antibodies. The myc antibody recognizes both MFH–FAR1 and GUS–FHY3, thus serving as a positive control, whereas the flag antibody only recognizes MFH–FAR1. The precipitates were subjected to western blot analyses probed with either a GUS antibody (Molecular Probes) for detecting the GUS–FHY3 fusion protein (upper panel) or a flag antibody (Sigma) for detecting the MFH–FAR1 fusion protein (lower panel). The asterisk indicates a possible degradation product of MFH–FAR1. T, total protein extracts; F_2, F_2 seedlings from a genetic cross between the GUS–FHY3 and MFH–FAR1 transgenic lines; –Ab, the sample was processed for immunoprecipitation without adding any antibody.

Discussion

The genetically identified phytochrome A signaling components in Arabidopsis do not define a simple linear pathway

The *FHY3* gene was identified in a genetic screen for mutants displaying specific defects in FRc inhibition of hypocotyl elongation (Whitelam *et al*., 1993). The *fhy3* mutant displays an elongated hypocotyl specifically under FRc. This FRc phenotype is not due to reduced levels of active phyA or to a deficiency in chromophore biosynthesis (Whitelam *et al*., 1993). Thus, FHY3 is likely to represent an authentic signaling transducer for phyA. Interestingly, loss-of-function mutants (presumably null mutant alleles) of *FHY3* and several other positively acting phyA signaling components only exhibited partial defects with different spectra and strengths in phyA signaling, suggesting that phyA signaling involves multiple branches or parallel pathways. *fhy3*, *fhy1*, *pat1* and *fin2* mutants display similar defects in various FRc responses, including inhibition of hypocotyl growth, apical hook and cotyledon opening, anthocyanin accumulation and FRc preconditioned blocking of greening. They also affect the induction of *RBCS* and *CHS* by FRc (Barnes *et al*., 1996a; Soh *et al*., 1998; Bolle *et al*., 2000; Yanovsky *et al*., 2000; Figure 3A),

indicating that these loci act early in phyA signaling. However, although the *fhy3* mutants are severely impaired in the above listed FR–HIR responses, they largely retain VLFR, which is defective in the *fhy1-1* and the *phyA* photoreceptor mutants (Yanovsky *et al*., 2000). Thus, *FHY3* and *FHY1* are likely to represent two different branch points in the phyA signaling. Consistent with this notion, the repression of *PORA* gene expression is obviously defective in *phyA-1* and *fhy1-1*, but appears normal in *fhy3* (Figure 3A). The repression of *PORA* by FRc has been proposed to be responsible for the loss of FRc preconditioned greening block in the *fhy1* and *phyA* mutants (Barnes *et al*., 1996b). Therefore it seems that *fhy3* may utilize a distinct mechanism to regulate the PORA protein level which might be responsible for the loss of FRc preconditioned greening block in this mutant. It will be interesting to examine both the transcript and protein levels of *PORA* in *fhy3*, *fin2* and *pat1*, which may clarify this issue.

fin219 and *far1* differ from the above mutants in that cotyledon opening and expansion as well as the FRc preconditioned greening block are not affected, although they are defective in hypocotyl elongation and anthocyanin accumulation (Hudson *et al*., 1999; Hsieh *et al*., 2000). The induction of *RBCS* and *CHS* by FRc is minimally affected in *far1-2* but is severely attenuated in *fin219* (Figure 3A), indicating that they represent close but different branches in phyA signaling. Although the phenotype of the *laf6* mutant seems most similar to that of *fin219* and is defective in both hypocotyl elongation and the induction of *CHS* (Møller *et al*., 2001), their different subcellular localizations suggest that they function at different steps in phyA-mediated signaling. HFR1 primarily affects the elongation and gravitropic response of the hypocotyl, whereas other FRc responses, including anthocyanin accumulation, FRc preconditioned block of greening and induction of *CHS*, are unaffected in this mutant (Fairchild *et al*., 2000). Also, the *laf1* mutant is affected in a distinct subset of phyA-dependent responses, including hypocotyl elongation, FRc preconditioned block of greening, anthocyanin accumulation and induction of *CHS*, whereas the FR-dependent apical hook opening, cotyledon unfolding and expansion, and gravitropism are not altered (Ballesteros *et al*., 2001). Taken together, the available data support a view that phyA signaling involves distinct combinations of these phyA signaling intermediates for controlling overlapping yet distinctive sets of FRc responses.

The finding that the double mutants *fhy3-1/far1-2*, *fhy3-1/fhy1-1* and *far1-2/fhy1-1* all display more elongated hypocotyls, whereas the *fhy3-1/spa1-3* double mutant has a hypocotyl of intermediate length (Figure 1E–H), further indicates that there is no simple downstream/upstream relationship among these phyA signaling components. Instead, it suggests that a complex interactive network of these signaling components mediates phyA signaling. For example, non-allelic non-complementation between *fin2* and *fhy3-1* as well as between *fin219* and *fhy1* has been reported (Soh *et al*., 1998; Hsieh *et al*., 2000), indicating that their gene products may interact directly or engage in extensive cross-talk. Furthermore, the observed down-regulation of the *FHY3* transcript level in FRc-grown *fin219* and *spa1-3* seedlings, and the increased accumulation of *FHY3* transcript in *far1-2* seedlings (Figure 5A), suggest that the accumulation of the *FHY3* transcript is subject to both positive and negative feedback regulation by specific phyA signaling components, and that the co-action of these signaling components determines the ultimate *FHY3* expression level.

FHY3 and FAR1 constitute a key module in the phyA signaling process

The findings that *fhy3* and *far1* mutants display similar yet distinct phenotypes and that *FHY3* and *FAR1* encode two homologous proteins are particularly interesting. Both mutants display elongated hypocotyls and reduced anthocyanin accumulation. However, *fhy3* has a much more pleiotropic effect on phyA signaling. For example, apical hook and cotyledon opening, and FRc preconditioned block of greening are affected by *fhy3* but not by *far1*. The *fhy3-1/far1-2* double mutant displays a more etiolated phenotype than its respective single-mutant parents under FR, suggesting an additive effect of these two mutations. Moreover, overexpression of FAR1 or FHY3 can suppress the phenotype of each other's loss-of-function mutations. Furthermore, overexpression of partial fragments of FHY3 in the WT background causes reduced sensitivity to FRc in a dosage-dependent manner (Figure 6). Most strikingly, *Arabidopsis* seedlings homozygous for the transgene overexpressing the C-terminal portion of FHY3 (C473–839), which contains a coiled-coil domain, display an apparent complete loss of FRc responses, remarkably similar to *phyA* null mutants. This result indicates that the C-terminal fragment of FHY3 may interact with other intermediates of phyA signaling and that non-productive binding of this truncated FHY3 protein with its interactive partners could shut down the entire phyA signaling by a dominant-negative interference. This interference is substantially stronger than the effects of a *fhy3* null mutation and the *fhy3/far1* double mutant. Direct evidence for such a notion is provided by the demonstration that FHY3 and FAR1 directly interact with each other in a yeast two-hybrid assay and an *in vivo* co-immunoprecipitation assay. Furthermore, our data suggest that FHY3 and FAR1 are capable of homo- and/or hetero-interactions (Figure 7). The capacity for homo- or heterocomplex formation for both proteins presumably provides a great flexibility to integrate the varying signal imports through interactions with other components of the phyA signaling pathway. Therefore, FHY3, together with FAR1, constitutes a key module in a regulatory network mediating phyA signaling.

Although the exact biochemical functions of FHY3 and FAR1 are currently not known, their nuclear localization implies that they are most likely involved in regulation of gene expression. They could either directly bind to DNA to regulate gene expression similar to transcription factors, or interact with DNA–protein complex in a similar manner to co-activators or co-repressors. This scenario is consistent with the observation that light stimulates the formation of nuclear speckles for the phyA–GFP fusion protein (Kircher *et al*., 1999; Nagy *et al*., 2000), which may represent distinct protein complexes where phyA interacts with its partners to regulate gene expression directly on light-regulated promoter sequences. Evidence supporting such a view has been provided by the demonstrations that both the HFR1–PIF3 heterodimer and PIF3 homodimer

can bind preferentially to the Pfr form of phyA (Ni *et al*., 1999; Fairchild *et al*., 2000). Furthermore, it has been demonstrated that PIF3 could bind specifically to a G-box DNA sequence motif present in various light-regulated gene promoters (Martínez-Garcia *et al*., 2000). It is likely that FHY3 and FAR1 could, through their interactions with, or by modulation of, PIF3 and/or HFR1, regulate the PIF3 homodimer- or HFR1–PIF3 heterodimer-mediated FR light-specific gene expression. Determining whether FHY3/FAR1 homo- and heterocomplexes bind DNA directly or interact with phyA and/or other DNA-binding transcription factors (such as PIF3, HFR1 and HY5) to impose their regulatory activities on these proteins will certainly enhance our understanding of the mechanisms of phyA signaling.

Materials and methods

Plant materials and growth conditions

The *fhy3-1* mutant has been described previously (Whitelam *et al*., 1993). *fhy3-2* was isolated by screening a T-DNA mutated *Arabidopsis* population generated by Steve Dellaporta's laboratory at Yale University (ecotype *COL*; Galbiati *et al*., 2000). *fhy3-3* was isolated by screening the Feldmann's T-DNA population under FRc condition (ecotype WS); *fhy3-4* to *fhy3-10* were isolated during the *far1* mutant screen (Hudson *et al*., 1999) and kindly provided by Dr Quail's group (*No-0* ecotype).

Allelism of these mutations was determined by standard genetic crossing. Other mutant plants used in this study included *phyA-1*, *fhy1-1*, *phyB(hy3)*, *phyA/B* and *hy5-1* (all ecotype *Ler*); *fin219* (ecotype *COL*); *spa1-3* (ecotype *RLD*); *far1-2* (ecotype *No-0*) (Whitelam *et al*., 1993; Hoecker *et al*., 1998; Hsieh *et al*., 2000). Double mutants were constructed by crossing their respective parental mutations. Putative double mutants were selected from FRc-grown F_2 seedlings and backcrossed to their respective parental mutants to confirm their genotypes.

Surface sterilization and cold treatment of the seeds, and seedling growth conditions for different light sources were described previously (Hsieh *et al*., 2000). Seedlings were grown on GM agar plates containing 0.3% sucrose for mutant screening and phenotypic analysis. For hypocotyl length measurements, 20–30 seedlings for each genotype were measured under a dissecting microscope with a ruler.

RNA gel blot analysis

Total RNA was isolated from 4-day-old seedlings using the Qiagen RNeasy Plant Mini prep kit. The seedlings were grown under darkness or FRc for 4 days. For the light shift experiment, the seedlings were grown under darkness for 4 days prior to illumination with 4 h of FRc or R. Ten micrograms of total RNA were loaded onto the gel and blotted to nylon membrane. The *CHS* probe was derived from a 0.9 kb *Eco*RI fragment containing the *Arabidopsis CHS* coding region (Hsieh *et al*., 2000). The *RBCS* probe has been described previously (Torii *et al*., 1999). The *PORA* gene probe was a 580 bp genomic fragment generated by PCR using primers CGCGACTTCAACTCCATCAG and GGATCCAACAATGATG. The *FHY3* probe was derived from an *Eco*RI fragment of the cDNA clone. Equal loading of RNA was verified by ethidium bromide staining as well as by rehybridizing the blots with an 18S rDNA probe (Deng *et al*., 1991). Probes were labeled by random priming. Hybridization and washing were conducted according to a standard method (Deng *et al*., 1991).

Positional cloning of FHY3 and sequence analysis

For generating the mapping population, the *fhy3-2* allele (ecotype *COL*) was crossed with the *Ler* wild type. Long-hypocotyl seedlings under FRc light were selected in the F_2 generation and transferred to soil for growth. A total of ~2200 recombinant chromosomes were used for fine-mapping analysis. After the *FHY3* gene was narrowed down to a single BAC clone (F2F24), this BAC clone was used to screen the cDNA libraries (CD4-13 through CD4-16 combined) obtained from ABRC. A total of 22 cDNA clones representing four different genes were isolated. A full-length cDNA clone (14) for *FHY3* was sequenced and verified by sequencing the genomic region of eight different *fhy3* alleles and their corresponding ecotypes (Table I).

Recombinant plasmids for plant transformation

To generate a c-myc epitope (MEQKLISEEDL)-tagged FHY3, the N-terminal *Bam*HI–*Bgl*II fragment of the *FHY3* cDNA clone (14) was replaced by a PCR fragment using primers CACGGATCCATGGAACAGAAGCTTATTAGCGAAGAAGACCTTGACGAAACTAGTATGGATATAGACCTTCGACTACATTCAGGTGACCTTTGCAAAGGAGATGATGAG and CTGATCATCGCCCAGATCTACTGC to generate a modified full-length *FHY3* cDNA clone (designated 14A1A) with the added c-myc epitope at the N-terminus. Then a *Bam*HI–*Sal*I fragment containing the full-length *FHY3* coding region was cloned into the same sites of the binary vector pZPY122 (Serino *et al*., 1999), thus placing the *FHY3* gene under the control of the 35S promoter. This clone was designated *myc-FHY3*.

The N-terminal fragment of *FHY3* was deleted from *myc-FHY3* by digesting with *Spe*I and re-ligating to generate the N-terminal deletion construct (designated *myc-FHY3C473–839*). The C-terminal fragment of *FHY3* was deleted by digesting *myc-FHY3* with *Avr*II and *Sal*I, filling in both ends and re-ligating to generate the C-terminal deletion construct (designated *myc-FHY3N1-541*).

For localization of the FHY3 protein, a *Bam*HI–*Bgl*II fragment containing the 35S promoter and the *GUS* gene coding region was derived from the *pPZP222-GUS-m/hCOP1* construct (Wang *et al*., 1999) and cloned into the *Bam*HI site of *myc-FHY3* in the correct orientation to generate a construct designated *GUS-FHY3* (in which the *GUS* gene is fused in-frame with the N-terminus of the *myc-FHY3* transgene).

Two primers (CGCGGATCCAATTGCGGATGGATTTGCAAGAGAATCTGGTTAGTGATGC and GCGCTCGAGACATCTTGTCATTGCAACTCAGCTCCATG) were used in an RT–PCR reaction to obtain the full-length *FAR1* gene cDNA, and the PCR product was cloned into the TA cloning vector Topo 2.1 (Invitrogen) to generate the clone *TA-FAR1*. A *Bam*HI–*Sal*I fragment containing the full-length *FAR1* coding region was released from *TA-FAR1* and cloned into the *Bam*HI–*Xho*I sites of the binary vector pZPY112 (Serino *et al*., 1999) to generate a construct named *pZPY112-FAR1* (in which the *FAR1* gene is driven by the 35S promoter).

To generate a myc-flag-HA epitope-tagged *FAR1* gene construct in the binary vector, two complementary oligos (CTAGAATGGAACAGAAGCTTATTAGCGAAGAAGACCTTGACGTCGACTACAAAGACGATGACGATAAAGCATACCCATATGACGTACCGGATTACGCAAG and GATCCTTGCGTAATCCGGTACGTCATATGGGTATGCTTTATCGTCATCGTCTTTGTAGTCGACGTCAAGGTCTTCTTCGCTAATAAGCTTCTGTTCCATT) were annealed *in vitro* by mixing together in 1× *Taq* polymerase buffer and heating to 70°C for 30 min, then slowly cooling to room temperature. The annealing product was ethanol precipitated and resuspended in water. The resulting double-stranded DNA (coding for the myc-flag-HA epitope) has ready-to-ligate restriction sites at both ends (*Xba*I at one end, *Bam*HI at the other) and was ligated into the *Xba*I–*Bam*HI sites of the binary vector clone *pZPY112-FAR1* to generate a clone termed *MFH-FAR1*.

All the above constructs were sequence confirmed. Those binary vector constructs were electroporated into the *Agrobacterium* strain GV3101 and used to transform *Arabidopsis*. Transgenic plants containing transgenes from the pZPY122 vector were selected with gentamycin (100 μg/ml). Transgenic plants derived from pZPY112 vector constructs were selected with kanamycin (50 μg/ml).

A total of ~30 independent T_1 transgenic plants were selected and grown to T_2 generation for each plant transformation construct. Drug-resistance tests were conducted for each T_2 transgenic line to determine the number of T-DNA insertions. Phenotype analysis was conducted with single T-DNA insertion lines. For each construct, the transgenic plant phenotypes reported here were observed in at least three independent lines examined.

Yeast two-hybrid assay

All LexA fusion constructs were cloned as a translational fusion to the LexA DNA-binding domain of vector pEG202, and all activation domain fusions were cloned in-frame with the HA-tagged GAL4 acidic activation domain of vector pJG4-5 (Torii *et al*., 1998). For the *FHY3* gene, the N-terminal *Bam*HI–*Bgl*II fragment of the *FHY3* cDNA clone was replaced by a PCR fragment using primers CCGAATTCGGATCCATGGATATAGACCTTCGACTACATTCAGG and CTGATCATCGCCCAGATCTACTGC. This modified *FHY3* cDNA cloned was termed *14F1*, in which an internal *Bgl*II site was mutated without changing the amino acid sequence of this fragment, which facilitated downstream

cloning efforts. An *Eco*RI fragment containing the N-terminal 250 amino acids of *FHY3* was cloned into the *Eco*RI site of pEG202 and pJG4-5 vectors in the correct orientation to generate *LexA-FHY3N* and *AD-FHY3N*. Then a *Xho*I fragment overlapping with the N-terminal portion of *FHY3* and containing the remaining cDNA of *FHY3* was cloned into *Xho*I-digested *LexA-FHY3N* and *AD-FHY3N* in the correct orientation to generate *LexA-FHY3* and *AD-FHY3*, both of which contain the full-length *FHY3* gene. A *Bam*HI–*Sal*I fragment containing the C-terminal amino acids 541–839 of *FHY3* was generated via PCR using the *FHY3* cDNA clone (14) as a template and the primers GGGATCCGACCTCGA-GATCCTAGGGAGGAGAACCGAGATGCCACATGT and the T7 primer. This PCR product was cloned into the *Bam*HI–*Sal*I sites of the pEG202 to generate *LexA-FHY3C*. Then, an *Eco*RI fragment containing the insert was released from this construct and cloned into the *Eco*RI site of pJG4-5 to generate *AD-FHYC*. For the *FAR1* gene, a *Bam*HI–*Xho*I fragment containing the full-length *FAR1* cDNA was released from the clone *TA-FAR1* and ligated into the *Bam*HI–*Xho*I sites of pEG202 to generate *LexA-FAR1*. A *Mfe*I–*Xho*I fragment containing the full-length FAR1 coding region was released from *TA-FAR1* and cloned into the *Eco*RI–*Xho*I sites of pJG4-5 to generate *AD-FAR1*. Yeast transformation, mating and liquid assay were conducted as described in Ausubel *et al*. (1999).

Immunoprecipitation

Light-grown WT and F_2 seedlings of a cross between the GUS–FHY3 and MFH–FAR1 transgenic lines were processed for co-immunoprecipitation assay in a buffer containing 50 mM Tris pH 7.5, 150 mM NaCl, 10 mM $MgCl_2$, 0.1% NP-40, 1 mM PMSF and 1× complete protease inhibitors (Roche). Either a myc- or a flag-epitope antibody and protein A–agarose beads (Sigma) were used to precipitate the immunoprotein complex. SDS–PAGE and western blotting analysis were performed according to standard procedures.

Acknowledgements

We thank Dr Garry Whitelam for the *fhy1-1* and *fhy3-1* mutant seeds, Dr Steve Delaporta for allowing us to screen the T-DNA mutated *Arabidopsis* population generated in his laboratory, Drs Rebecca Fry and Lay-Hong Ang for isolating the *fhy3-2* and *fhy3-3* alleles, respectively, and Dr Peter Quail for providing additional *fhy3* alleles (*fhy3-4* to *fhy3-10*) and the *far1-2*, *spa1-3* mutant seeds. We are also very thankful to Jie Liu and Anandasankar Ray for helping with the *FHY3* mapping. We are grateful to the *Arabidopsis* Biological Resource Center (ABRC; Ohio State University, Columbus) for DNA markers, cDNA library and BAC clones. We also thank Timothy Nelson and Jessica Habashi for reading and critical comments on the manuscript. This work was supported by grants from the NIH (GM47850) and Human Frontier Science program and a NSF presidential Faculty Fellow Award (to X.W.D). H.W. is an NIH postdoctoral fellow (1-F32-GM20540-01).

References

Ausubel,F., Brent,R., Kingston,R.E., Moore,D.D., Seidman,J.G., Smith, J.A. and Struhl,K. (1999) *Short Protocols in Molecular Biology*. John Wiley and Sons, New York, NY.

Ballesteros,M., Bolle,C., Lois,L.M., Moore,J.M., Vielle-Calzada,J.-P., Grossniklaus,U. and Chua,N.-H. (2001) LAF1, a MYB transcription activator for phytochrome A signaling. *Genes Dev.*, **15**, 2613–2625.

Barnes,S.A., Quaggio,R.B., Whitelam,G.C. and Chua,N.-H. (1996a) *fhy1* defines a branch point in phytochrome A signal transduction pathways for gene expression. *Plant J.*, **10**, 1155–1161.

Barnes,S.A., Nishizawa,N.K., Quaggio,R.B., Whitelam,G.C. and Chua,N.-H. (1996b) Far-red light blocks greening of *Arabidopsis* seedlings via a phytochrome A-mediated change in plastid development. *Plant Cell*, **8**, 601–615.

Bell,C.J. and Ecker,J.R. (1994) Assignment of 30 microsatellite loci to the linkage map of *Arabidopsis*. *Genomics*, **19**, 137–144.

Bolle,C., Koncz,C. and Chua,N.-H. (2000) PAT1, a new member of the GRAS family, is involved in phytochrome A signal transduction. *Genes Dev.*, **14**, 1269–1278.

Colón-Carmona,A., Chen,D.L., Yeh,K.-C. and Abel,S. (2000) Aux/IAA proteins are phosphorylated by phytochrome *in vitro*. *Plant Physiol.*, **124**, 1728–1738.

Deng,X.W. and Quail,P.H. (1999) Signalling in light-controlled development. *Semin. Cell Dev. Biol.*, **10**, 121–129.

Deng,X.W., Caspar,T. and Quail,P.H. (1991) *cop1*: a regulatory locus involved in light-controlled development and gene expression in *Arabidopsis*. *Genes Dev.*, **5**, 1172–1182.

Desnos,T., Puente,P., Whitelam,G.C. and Harberd,N.P. (2001) FHY1: a phytochrome A-specific signal transducer. *Genes Dev.*, **15**, 2980–2990.

Dieterle,M., Zhou,Y.-C., Schäfer,E., Funk,M. and Kretsch,T. (2001) EID1, an F-box protein involved in phytochrome A-specific light signaling. *Genes Dev.*, **15**, 939–944.

Fairchild,C.D., Schumaker,M.A. and Quail,P.H. (2000) *HFR1* encodes an atypical bHLH protein that acts in phytochrome A signal transduction. *Genes Dev.*, **14**, 2377–2391.

Fankhauser,C. (2000) Phytochromes as light-modulated protein kinases. *Semin. Cell Dev. Biol.*, **11**, 467–473.

Galbiati,M., Moreno,M.A., Nadzan,G., Zourelidou,M. and Dellaporta,S.L. (2000) Large-scale T-DNA mutagenesis in *Arabidopsis* for functional genomic analysis. *Funct. Integr. Genomics*, **1**, 25–34.

Hoecker,U., Xu,Y. and Quail,P.H. (1998) *SPA1*: a new genetic locus involved in phytochrome A-specific signal transduction. *Plant Cell*, **10**, 19–33.

Hoecker,U., Tepperman,J.M. and Quail,P.H. (1999) SPA1, a WD-repeat protein specific to phytochrome A signal transduction. *Science*, **284**, 496–499.

Hsieh,H.-L., Okamoto,H., Wang,M., Ang,L.-H., Matsui,M., Goodman,H. and Deng,X.W. (2000) *FIN219*, an auxin-regulated gene, defines a link between phytochrome A and the downstream regulator COP1 in light control of *Arabidopsis* development. *Genes Dev.*, **14**, 1958–1970.

Hudson,M., Ringli,C., Boylan,M.T. and Quail,P.H. (1999) The *FAR1* locus encodes a novel nuclear protein specific to phytochrome A signaling. *Genes Dev.*, **13**, 2017–2027.

Hudson,M.E. (2000) The genetics of phytochrome signalling in *Arabidopsis*. *Semin. Cell Dev. Biol.*, **11**, 475–483.

Kircher,S., Kozma-Bognar,L., Kim,L., Adam,E., Harter,K., Schäfer,E. and Nagy,F. (1999) Light quality-dependent nuclear import of the plant photoreceptors phytochrome A and B. *Plant Cell*, **11**, 1445–1456.

Konieczny,A. and Ausubel,F.M. (1993) A procedure for mapping *Arabidopsis* mutations using co-dominant ecotype-specific PCR-based markers. *Plant J.*, **4**, 403–410.

Kuno,N. and Furuya,M. (2000) Phytochrome regulation of nuclear gene expression in plants. *Semin. Cell Dev. Biol.*, **11**, 485–493.

Ma,L., Li,J., Qu,L., Hager,J., Chen,Z., Zhao,H. and Deng,X.W. (2001) Light control of *Arabidopsis* development entails coordinated regulation of genome expression and cellular pathways. *Plant Cell*, **13**, 2589–2607.

Martínez-Garcia,J.F., Huq,E. and Quali,P.H. (2000) Direct targeting of light signals to a promoter element-bound transcription factor. *Science*, **288**, 859–863.

Møller,S.G., Kunkel,T. and Chua,N.-H. (2001) A plastidic ABC protein involved in intercompartmental communication of light signaling. *Genes Dev.*, **15**, 90–103.

Nagatani,A., Reed,J.W. and Chory,J. (1993) Isolation and initial characterization of *Arabidopsis* mutants that are deficient in phytochrome A. *Plant Physiol.*, **102**, 269–277.

Nagy,F., Kircher,S. and Schäfer,E. (2000). Nucleo-cytoplasmic partitioning of the plant photoreceptors phytochromes. *Semin. Cell Dev. Biol.*, **11**, 505–510.

Neff,M.M., Fanhauser,C. and Chory,J. (2000) Light: an indicator of time and place. *Genes Dev.*, **14**, 257–271.

Ni,M., Halliday,K.J., Tepperman,J.M. and Quail,P.H. (1999) Binding of phytochrome B to its nuclear signaling partner PIF3 is reversible by light. *Nature*, **400**, 781–784.

Quail,P.H. (2000) Phytochrome-interacting factors. *Semin. Cell Dev. Biol.*, **11**, 457–466.

Serino,G., Tsuge,T., Kwok,S., Matsui,M., Wei,N. and Deng,X.W. (1999) *Arabidopsis cop8* and *fus4* define the same gene that encodes subunit 4 of the COP9 signalosome. *Plant Cell*, **11**, 1967–1979.

Soh,M.S., Hong,S.H., Hanzawa,H., Furuya,M. and Nam,H.G. (1998) Genetic identification of *FIN2*, a far red light-specific signaling component of *Arabidopsis thaliana*. *Plant J.*, **16**, 411–419.

Torii,K.U., McNellis,T.W. and Deng,X.W. (1998) Functional dissection of *Arabidopsis* COP1 reveals specific roles of its three structural modules in light control of seedling development. *EMBO J.*, **17**, 5577–5587.

Torii,K.U., Stoop-Myer,C.D., Okamoto,H., Coleman,J.E., Matsui,M. and Deng,X.W. (1999) The RING-finger motif of photomorphogenic

repressor COP1 specifically interacts with the RING-H2 motif of a novel *Arabidopsis* protein. *J. Biol. Chem.*, **274**, 27674–27681.

Wang,H. and Deng,X.W. (2002) Phytochrome signaling mechanism. In Somerville,C. and Meyerowitz,E. (eds), *The Arabidopsis Book*, in press.

Wang,H., Kang,D., Deng,X.W. and Wei,N. (1999) Evidence for functional conservation of a mammalian homologue of the light-responsive plant protein COP1. *Curr. Biol.*, **9**, 711–714.

Whitelam,G.C., Johnson,E., Peng,J., Carol,P., Anderson,M.L., Cowl,J.S. and Harberd,N.P. (1993) Phytochrome A null mutants of *Arabidopsis* display a wild-type phenotype in white light. *Plant Cell*, **5**, 757–768.

Yanovsky,M.J., Casal,J.J. and Luppi,J.P. (1997) The *VLF* loci, polymorphic between ecotypes *landsberg erecta* and *Columbia*, dissect two branches of phytochrome A signal transduction that correspond to very-low-fluence and high-irradiance responses. *Plant J.*, **12**, 659–667.

Yanovsky,M.J., Whitelam,G.C. and Casal,J.J. (2000) *fhy3-1* retains inductive responses of phytochrome A. *Plant Physiol.*, **123**, 235–242.

Received November 26, 2001; revised January 16, 2002; accepted January 22, 2002